Research article

SURFACE and INTERFACE ANALYSIS

Received: 6 October 2010 Revised: 5 April 2011 Accepted: 23 May 2011 Published online in Wiley Online Library: 28 June 2011

(wileyonlinelibrary.com) DOI 10.1002/sia.3802

The interaction of CO_2 and CO with Fe-doped $SrTiO_3$(100) surfaces

F. Voigts,[a] Chr. Argirusis[b,c] and W. Maus-Friedrichs[a,d]*

The interaction of CO_2 and CO with 0.013 at.% Fe-doped $SrTiO_3$(100) was investigated *in situ* with Metastable Induced Electron Spectroscopy (MIES) and XPS at room temperature. To clear up the influence of surface defects, cleaned and sputtered $SrTiO_3$ surfaces were investigated. Sputtering results in the breaking of Ti–O bonds in the surface and the formation of oxygen-related defects as well as reduced titanium on the surface.

Cleaned $SrTiO_3$ surfaces do neither interact with CO_2 nor with CO. Sputtered surfaces show a CO_3^{2-} formation during CO_2 exposure and – to a lesser extent – during CO exposure. The CO_3^{2-} groups can be detected very well with MIES because of its extreme surface sensitivity. With XPS, the characteristic carbonate peak shift of the C 1s orbitals can be detected.

Keywords: MIES; UPS; XPS; strontium titanate; carbon dioxide; carbon monoxide

Introduction

$SrTiO_3$ has been studied for very different aspects in the last years. It is technologically important, for example, as high temperature oxygen sensor,[1] in photocatalysis, as substrate for high-T_c superconductors,[2,3] in capacitors and as dielectrical component.[4–7]

$SrTiO_3$ provides a remarkable thermal and chemical stability. It shows a perovskite structure which is stable between 105 and 2300 K without phase transitions, even for high doping concentrations. The ionic and electronic transport phenomena are frequently discussed on the basis of defect chemical descriptions.[8–10] Recently, a review was published by Merkle and Maier using Fe-doped $SrTiO_3$ as model material for the oxygen incorporation into oxides.[11]

The use of $SrTiO_3$ as an oxygen sensor at temperatures above about 700 K is based on the interaction of oxygen molecules with the surface of the material. This three-step process involves the dissociation of the impinging molecule at the surface, the incorporation of the adsorbed atoms into the surface and the subsequent diffusion into the bulk. The incorporation reaction is usually assumed to occur as follows:[12]

$$\frac{1}{2}O_2 + V_O^{\bullet\bullet} \Leftrightarrow O_O^{\times} + 2h^{\bullet} \quad (1)$$

In the equation, we use Kröger–Vink notation. The large characters represent the chemical species, the subscripts the lattice site and the superscripts the charge of the species. $O_O^{\times}$ stands for a regular lattice oxygen ion, $h^{\bullet}$ for an electronic hole and $V_O^{\bullet\bullet}$ for an oxygen vacancy. The superscripts $X^{\bullet}$, X' and $X^{\times}$ represent a single positive, single negative and a neutral charge with respect to the host lattice.

The possibility of cross-sensitivity of this reaction for other oxygen-containing gases has drawn increasing attention in the recent years. Cross-sensitivity means, that other oxygen-containing gases apart from O_2 can act as a source of oxygen for Eqn (1). One possibility is the substitution of O_2 by CO_2. It has already been shown with Isotope Exchange Depth Profiling (IEDP) and Temperature Programmed Desorption (TPD), that this is possible, most likely via the following pathway:[13]

$$CO_2 + V_O^{\bullet\bullet} \Rightarrow CO + O_O^{\times} + 2h^{\bullet} \quad (2)$$

This reaction does not produce any permanent adsorbates at the clean surface, as could be verified with Metastable Induced Electron Spectroscopy (MIES) and X-ray Photoelectron Spectroscopy (XPS). This behaviour has also been predicted by Density Functional Theory (DFT) calculations.[14]

Other authors also examined the interaction of CO_2 and CO with $SrTiO_3$ by means of TPD at low temperatures.[15] They found that the surface oxygen vacancies play an important role in the dissociation process. On surfaces with a high defect density, they observe total dissociation of the impinging molecules.

It is the aim of this work to contribute to the understanding of the fundamental interactions of CO_2 and CO molecules with $SrTiO_3$(100) surfaces at room temperature by means of electron spectroscopy. For this purpose, surfaces with high defect density were prepared by sputtering of the sample and compared to surfaces with low defect density.

Previous work on the interaction with water was published recently[16] which gives evidence that the $SrTiO_3$(100) surface

* *Correspondence to: W. Maus-Friedrichs, Institut für Physik und Physikalische Technologien, Technische Universität Clausthal, Leibnizstrasse 4, 38678 Clausthal-Zellerfeld, Germany. E-mail: w.maus-friedrichs@pe.tu-clausthal.de*

a *Institut für Physik und Physikalische Technologien, Technische Universität Clausthal, 38678 Clausthal-Zellerfeld, Germany*

b *School of Chemical Engineering, National Technical University of Athens, Zografou 15780, Athens, Greece*

c *Institut für Metallurgie, Technische Universität Clausthal, 38678 Clausthal-Zellerfeld, Germany*

d *Clausthaler Zentrum für Materialtechnik, Technische Universität Clausthal, 38678 Clausthal-Zellerfeld, Germany*

investigated here is at least mainly terminated by a TiO_2 layer. This applies for cleaned as well as for sputtered surfaces. For a detailed discussion on the surface termination the reader is referred to the corresponding literature.

Where applicable, results presented will act as the basis for the interpretation of results in this study: sputtering of the $SrTiO_3(100)$ surfaces results in the breaking of Ti–O bonds in the surface and the formation of oxygen-related defects ($V_O^{\bullet\bullet}$ and/or undercoordinated surface oxygen atoms), which can be detected with XPS. The breaking of the Ti–O bonds also produces reduced titanium $Ti_{Ti}^{'}$ on the surface, which is visible in MIES as reduced Ti 3d states within the band gap.

Experimental

An ultrahigh vacuum (UHV) apparatus with a base pressure of 5×10^{-11} mbar, which has been described in detail previously,[17] is used to carry out the spectroscopic measurements.

Electron spectroscopy is performed using a hemispherical analyzer (VSW HA100) in combination with a source for metastable helium atoms ($He^*\ ^3S_1$) and ultraviolet photons (HeI line). A commercial non-monochromatic X-ray source (Specs RQ20/38C) is utilized for XPS. A commercial LEED system (Physical Electronics 11–020) is used for the investigation of the surface structure.

During XPS, X-ray photons hit the surface under an angle of 80° to the surface normal, illuminating a spot of several mm in diameter. For all measurements presented here, the Al K_α line with a photon energy of 1486.7 eV is used. Electrons are recorded by the hemispherical analyzer with an energy resolution of 1.1 eV under an angle of 10° to the surface normal. All XPS spectra are displayed as a function of binding energy with respect to the Fermi level. As we do not discuss absolute binding energy values, we do not correct the spectra for binding energy shifts.

For quantitative XPS analysis, photoelectron peak areas are calculated via mathematical fitting with Gauss-type profiles using OriginPro 7G including the PFM fitting module, which uses Levenberg–Marquardt algorithms to achieve the best agreement possible between experimental data and fit. Photoelectric cross-sections as calculated by Scofield[18] and inelastic mean free paths from the NIST database[19] as well as the transmission function of our hemispherical analyzer are taken into account when calculating stoichiometry.

The MIES is performed by applying a cold cathode gas discharge via a two-stage pumping system. A time-of-flight technique is employed to separate electrons emitted by He* from those caused by HeI interaction with the surface. The combined He*/HeI beam strikes the sample surface under an angle of 45° to the surface normal and illuminates a spot of approximately 2 mm in diameter. The spectra are recorded simultaneously by the hemispherical analyzer with an energy resolution of 220 meV under normal emission within 280 s.

MIES is an extremely surface-sensitive technique probing solely the outermost layer of the sample, because the He* atoms interact with the surface typically 0.3 to 0.5 nm in front of it. This may occur via a number of different mechanisms depending on surface electronic structure and work function (WF), which are described in detail elsewhere.[20–22]

On $SrTiO_3$ surfaces a special Auger Deexcitation (AD) type interaction occurs.[23] The 2s electron of the impinging He* is resonantly transferred into the surface of the sample and localizes at near surface Ti 3d states. Subsequently, a Ti 3d electron fills the hole in He^+ 1s in an interatomic Auger neutralization (AN) process, followed by the emission of an O 2p surface electron carrying the excess energy. The energy of the resulting MIES peak is shifted towards higher binding energies compared to conventional AD due to a diminished local ionization potential.

All MIES spectra are displayed as a function of the electron binding energies with respect to the Fermi level. The surface WF can be determined from the high binding energy onset of the MIES spectra with an accuracy of ±0.1 eV.

For all experiments, 0.013 at.% Fe-doped $SrTiO_3$ is mounted in a sample manipulator by means of a molybdenum holder and introduced into the UHV as received from the supplier (Crystec GmbH Berlin, Verneuil growth method). The holder is fitted with a backside electron bombardment sample heating system. Prior to the experiments the sample is annealed at 970 K in the UHV for about 2 h, the oxygen partial pressure is well below 10^{-13} mbar during this procedure as measured by quadrupole mass spectrometry. This is done to clean the surface from adsorbates and to produce oxygen bulk vacancies. With this procedure a sufficient number of vacancies could be produced to achieve the necessary crystal conductibility for electron spectroscopy. After this initial treatment, the sample is kept under UHV conditions and is cleaned directly prior to every experiment by short annealing to about 800 K. The surfaces prepared in this manner are referred to as 'cleaned' surfaces in the following.

Sputtering of the samples is achieved by means of a Leybold-Heraus IQP 10/63 penning ion source, which is mounted in a preparation chamber directly adjacent to the analysis chamber, using argon ions as projectiles. For the sputtering procedures discussed here, ion energies of 3 keV and fluxes of about 8 μA were used. The sputter rate was identified by masking and subsequent measuring with a profilometer and amounts to about 0.008 nm s^{-1}. According to Leybold–Heraeus, the ion beam intensity is distributed uniformly across our sample with a constant flux. The sample is treated for 300 s for all experiments, which results in a mean sputter depth of about 2.4 nm. All samples were cleaned prior to sputtering as described in the preceding paragraph. Directly after sputtering, adsorbates from the residual gas in the preparation chamber are removed from the surface by cautious annealing to 560 K. During this annealing process, the surface density of states of states is under continuous control of the MIES spectrometer to make sure that it does not remove sputter-induced defects from the surface.[16] In this way, it can also be verified that the surface is free from surface OH groups or other adsorbates after annealing. The surfaces prepared in this manner are referred to as 'sputtered' surfaces in the following.

CO_2 and CO are offered via backfilling the chamber using a bakeable leak valve. The gas line is evacuated and can be heated in order to ensure cleanness. A quadrupole mass spectrometer (Balzers QMS 112A) is used to monitor the partial pressure of the gases during experiments simultaneously to the MIES measurements.

All measurements shown here are performed at room temperature, except otherwise stated.

Results

CO_2 on cleaned $SrTiO_3$

Figure 1 shows a set of MIES spectra gathered from a $SrTiO_3(100)$ surface. The first spectrum is displayed at the bottom and shows the

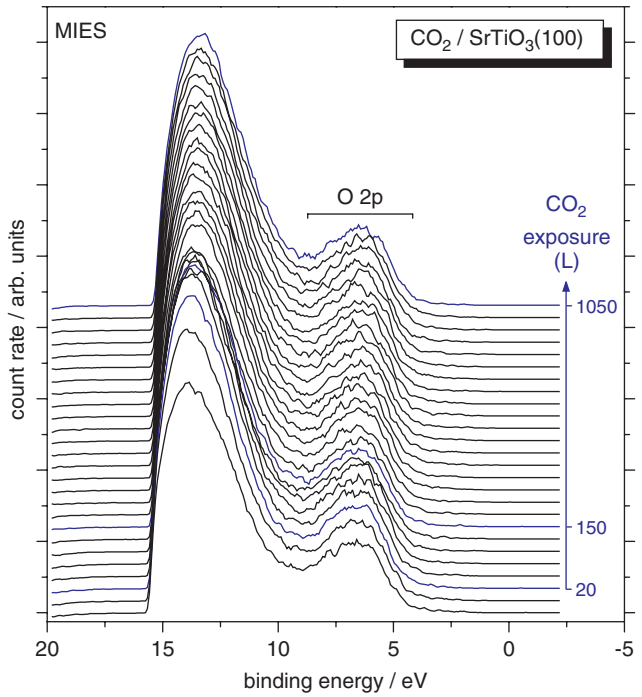

Figure 1. MIES spectra of cleaned $SrTiO_3$(100) during CO_2 exposure.

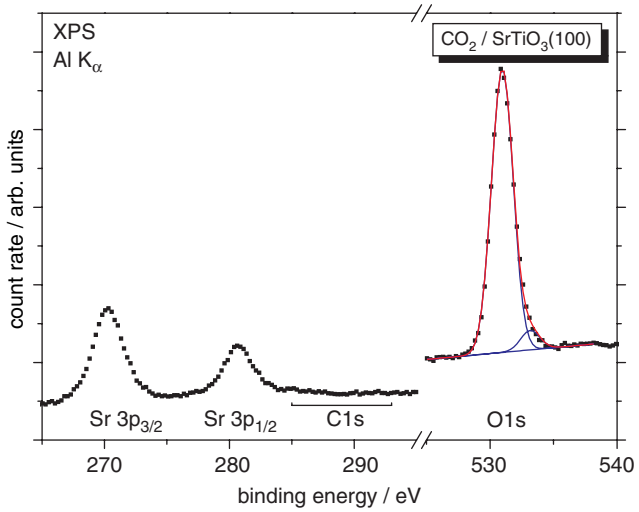

Figure 2. XPS spectrum of cleaned and CO_2 exposed $SrTiO_3$(100) (corresponding to the top MIES spectrum in Fig. 1) from the Sr 3p, C 1s and O 1s region. The exposure amounts to 1050 L CO_2.

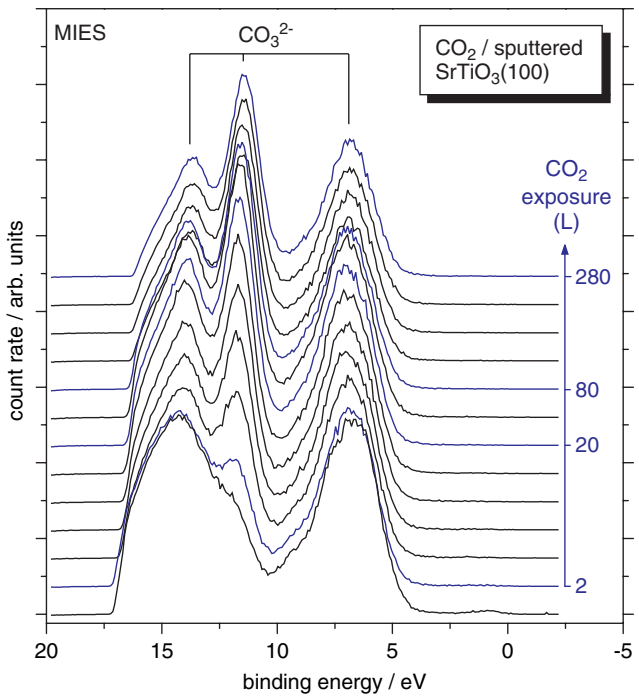

Figure 3. MIES spectra of sputtered $SrTiO_3$(100) during CO_2 exposure.

cleaned surface, prepared as described in the preceding section. The subsequent spectra are shown offset above the first one.

The strong increase in intensity around 15 eV is due to secondary electrons and will not be discussed. The peak at 6.5 eV originates from electrons emitted from O 2p-derived states in the $SrTiO_3$ surface as described in the experimental. The spectrum resembles the well-known surface density of states of the sample.[16,23]

Beginning with the third spectrum, CO_2 was offered to the surface, with the exposure indicated by the arrow on the right side. Although the CO_2 exposure was as high as 1050 L at the end of the experiment, it does not change the spectrum, indicating that the surface electronic structure is unchanged. Obviously, no interaction between the surface and the CO_2 is detectable with MIES. This behaviour has been reported previously.[13]

A XPS spectrum from the Sr 3p, C 1s and O 1s regions of the same sample is shown in Fig. 2. It was collected immediately after the top spectrum of Fig. 1. Between 265 and 285 eV emission from Sr 3p states is observed. Both the Sr $3p_{3/2}$ as well as the Sr $3p_{1/2}$ features display only one contribution at 270.3 and 280.7 eV due to regular lattice Strontium $Sr_{Sr}^{\times}$. The same holds for Titanium $Ti_{Ti}^{\times}$ (at 459.7 and 465.3 eV, not shown here).

In the region from 528 to 535 eV, emission from O 1s states is displayed. The peak consists of two contributions at 531.0 and 533.2 eV illustrated by the two Gaussians in blue, while their sum is shown as the thick red line. The experimental data are drawn as black squares. For the mathematical fitting procedure constraints from preliminary experiments are used. A full width at half maximum (FWHM) of 2.1 eV is employed for the first Gaussian. It is due to lattice oxygen $O_O^{\times}$, while the latter is attributed to surface oxygen and oxygen-related surface defects.[16] The second peak contributes with 4.3% to the total O 1s intensity.

Photoemission from C 1s orbitals should be observed in the interval from 285 to 293 eV electron binding energy, typically. The missing intensity in this interval reveals the number of carbon atoms in the surface is below the detection limit. With our setup, even small amounts of adsorbates on top of the $SrTiO_3$ surface can be detected easily.[16] Thus, this result backs up the results from the preceding MIES experiment. With XPS, no interaction process with CO_2 can be observed at this surface, although this does not rule out surface interactions completely.

CO_2 on sputtered $SrTiO_3$

In Fig. 3, a corresponding experiment is shown. The bottom MIES spectrum shows the sputtered surface, prepared as described in the experimental section. Compared to the cleaned surface from Fig. 1, additional intensity in the band gap just below the Fermi level is observed, although exhibiting a very small count

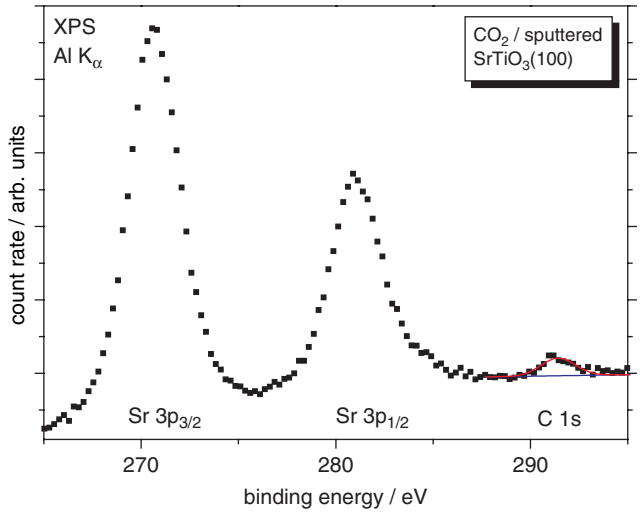

Figure 4. XPS spectrum of sputtered and CO_2 exposed $SrTiO_3(100)$ (corresponding to the top MIES spectrum in Fig. 3) from the Sr 3p and C 1s region. The exposure amounts to 280 L CO_2.

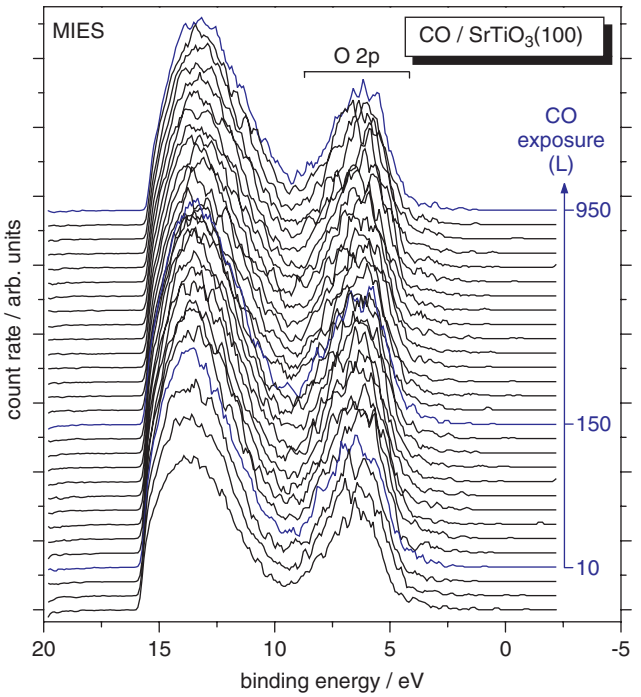

Figure 5. MIES spectra of cleaned $SrTiO_3(100)$ during CO exposure.

rate. This is attributed to sputter-induced surface defects due to emission from reduced Ti 3d states Ti'_{Ti}. As sputtering the surface results in the breaking of surface Ti–O bonds, these are assumed to be connected to oxygen vacancies $V_O^{\bullet\bullet}$.[16] Furthermore, a small peak around 12 eV can be detected, which is caused by surface contaminations, most probably involving OH groups. These contaminations are remnants from the sputter process and can not be avoided completely because of the enhanced surface reactivity of the sputtered $SrTiO_3$ to water.[16] Besides these two additional features, the surface resembles the cleaned surface from Fig. 1.

CO_2 is offered to the surface beginning with the second spectrum. Contrary to the experiment on cleaned $SrTiO_3$, a strong change in the spectra can be observed during CO_2 exposure. The main peak at 6.7 eV is diminished, while two additional contributions at 11.5 and 13.9 eV appear in the spectrum. The emission from Ti 3d states in the band gap is reduced to zero very quickly. 280 L of CO_2 have been offered to the surface until the end of the experiment. At this point, a constant three-peak structure has developed. A structure like this has been observed previously with MIES, for example, with CO_2 on calcium films.[24] It corresponds to a surface carbonate. The three peaks can be attributed to the molecular orbitals $1a'_2$, $1e'$, $4e'$ (6.7 eV); $3e'$, $1a'_2$ (11.5 eV) and $4a'_1$ (13.9 eV) of CO_3^{2-}.[25] This assignment of the registered MIES peaks to surface molecular orbitals has been proven to be very reliable in the past, although care must be taken when doing so for photoelectron spectroscopy on $SrTiO_3$.[14] Of course, this surface carbonate does not have to be in the same configuration as a regular bulk carbonate.

The formation of a surface carbonate on the $SrTiO_3$ can be confirmed with XPS. A corresponding spectrum collected immediately after the top spectrum in Fig. 3 is shown in Fig. 4. The two peaks from emission of Sr 3p orbitals resemble the maxima in Fig. 2, now detectable at 270.6 and 280.9 eV. At a binding energy of 291.4 eV, an additional feature denoted as C 1s can be observed. This binding energy roughly matches values measured for different carbonates, for example, on alkaline earth carbonates[26] and is significantly higher than what has been reported for 'carbonate-like CO_2 adsorbates' on low-defect surfaces.[14] A direct comparison of the binding energy values is difficult, because the carbonate chemical shift is different for different substrates and because different methods of binding energy-scale corrections are used in different studies. However, C 1s contributions beyond 290 eV electron-binding energy are attributed either to carbonates or fluorides usually. Emission from fluorine orbitals is not observed in Fig. 4.

CO on cleaned $SrTiO_3$

In Fig. 5, an experiment very similar to the one in Fig. 1 is shown. The bottom spectrum shows a cleaned $SrTiO_3(100)$ surface with the well-known surface density of states of the sample. During the collection of the subsequent spectra, the sample is exposed to CO. At the end of the experiment, the exposure amounts to 950 L. Similar to the exposure to CO_2, no changes can be observed in the spectra, indicating no interaction between the CO molecules and the surface does occur.

This conclusion can be backed up by the XPS analysis shown in Fig. 6, which was collected immediately after the top MIES spectrum in Fig. 5. In the region between 285 and 293 eV, no emission due to C 1s electrons is to be seen. The spectrum only displays the Sr 3p emission at 270.3 and 280.6 eV. Thus, the surface is free of carbon atoms after dosing CO.

XPS spectra from the O 1s region (not shown here) show a secondary contribution at 533.3 eV, which is due to surface oxygen and oxygen-related surface defects, that amounts to 4.6% of the total O 1s intensity. That is very similar to the results from Fig. 2.

CO on sputtered $SrTiO_3$

CO exposure to the sputtered $SrTiO_3(100)$ surface is shown in Fig. 7. The bottom spectrum resembles the sputtered surface from Fig. 3, with two additional features compared to the cleaned surface. At 12 eV and just below the Fermi level the features due to OH contamination and surface defects can be detected again.

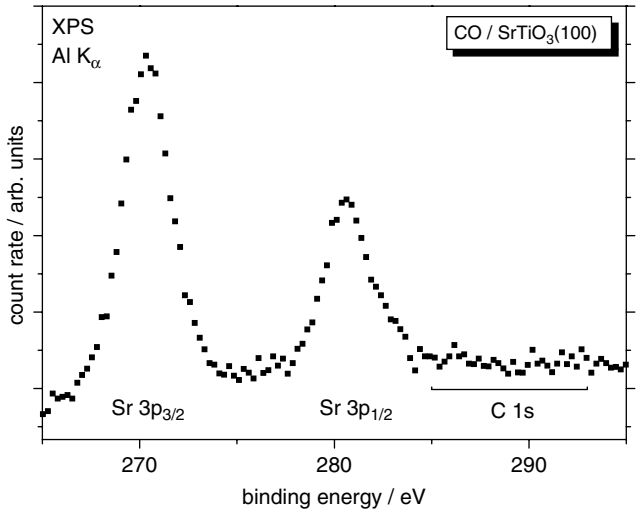

Figure 6. XPS spectrum of cleaned and CO exposed $SrTiO_3$(100) (corresponding to the top MIES spectrum in Fig. 5) from the Sr 3p and C 1s region. The exposure amounts to 950 L CO.

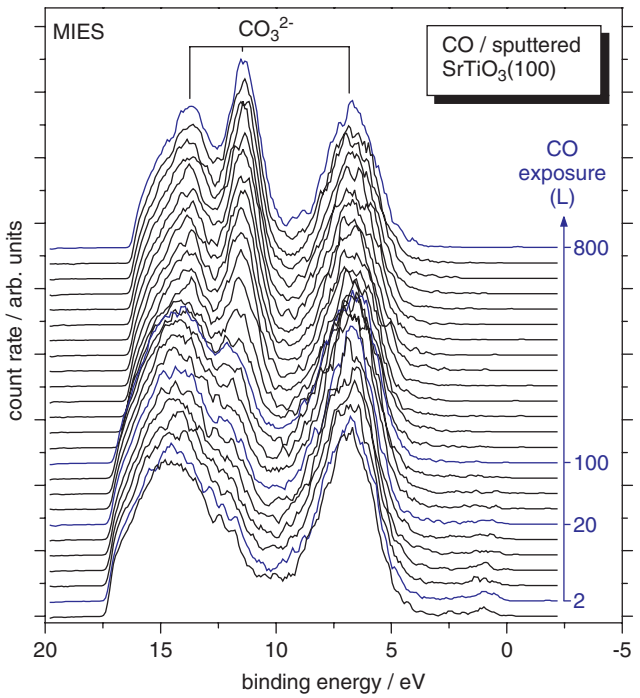

Figure 7. MIES spectra of sputtered $SrTiO_3$(100) during CO exposure.

Beginning with the second spectrum, CO was offered to this surface. Contrary to the experiments on the cleaned surface, a strong change in the subsequent spectra can be observed. The main peak at 6.8 eV due to emission from O 2p-derived orbitals is reduced, while two additional peaks at 11.5 and 13.7 eV develop. Emission from Ti 3d states in the band gap vanishes very quickly. At the end of the experiment, the spectrum resembles the top spectrum from Fig. 3 very much. The exposure amounts to 800 L CO at this point.

A molecular adsorption of the CO molecules does not occur. This would be visible by the presence of a distinct two peak structure due to ionization of the CO $1\pi/5\sigma$ and CO 4σ molecular orbitals, which cannot be observed here.[27]

The formation of a surface carbonate from the CO offer can be evidenced in the same way as for the CO_2 offer. The XPS analysis in Fig. 8 exhibits an additional feature at 291.5 eV. Again, this is evidence to the presence of a carbonate at the surface.

The secondary peak in the O 1s region in XPS (at 534.0 eV, not shown here), which is attributed to surface oxygen and oxygen-related surface defects, amounts to 9.3% of the total O 1s intensity. That is more than double the proportion than observed at the cleaned, unsputtered surface. Although the error in this calculation must be assessed to be quite high, it is sure to draw from this that the amount of surface defects is higher.

The MIES experiments in Figs 3 and 7 are further analyzed in Fig. 9. The peak height of the central CO_3^{2-} peak at 11.5 eV is plotted as a function of the gas exposure for the sputtered $SrTiO_3$(100) surface exposed to CO_2 and CO, respectively. For this analysis, the peak area of the central CO_3^{2-} peak was calculated after a subtraction of the secondary electron background. For better comparability, the plot for the CO exposed surface is magnified by a factor of 20. Additionally, the surface WF of the sputtered $SrTiO_3$(100) surface exposed to CO_2 and CO is shown.

Discussion

The experiment with CO_2 involving the cleaned $SrTiO_3$(100) surface does affirm previous results: with MIES and XPS, no change in the surface electronic structure or stoichiometry can be observed.

This does not rule out surface interactions completely, as has been pointed out in the introduction. The oxygen incorporation as per Eqn (2) does not back up the expectation of a change in the surface electronic structure itself. Quite the contrary, reaction (2) does only consume oxygen vacancies and produces CO. Both would neither be detectable with MIES nor with XPS: the CO is desorbed into the vacuum immediately and the time it stays at the surface is too short to make it detectable with electron spectroscopy. The change in surface oxygen vacancy density cannot be detected or at least not with sufficient accuracy to draw any conclusions.

In previous works on TiO_2(110) surfaces also no interaction of the CO_2 with the surface was reported.[28,29] As the $SrTiO_3$(100) used for the present study is TiO_2-terminated, this may support this conclusion, although new DFT calculations yield different results.[14] Of course, this is only true for room temperature experiments. Investigations at reduced temperatures have revealed other mechanisms.[28–30]

The experiments with CO at the cleaned surface yields the same outcome: no change in the surface electronic structure or stoichiometry can be observed with the methods applied. This does not answer the question if CO may be a source of oxygen for the incorporation into the $SrTiO_3$ in a similar way CO_2 is as per Eqn (2). This will be figured out with future IEDP experiments. A dissociation of the CO molecules in front of the surface would provide oxygen for an incorporation process similar to Eqn (1), but it would also produce surface carbon atoms from the process. Such remnants could not be detected in this study (Fig. 6).

Comparing the XPS results from the O 1s region of the cleaned surfaces in Fig. 2 to the sputtered surfaces in Figs 6 and 8, the strong increase in intensity of the secondary maximum from the sputter process is very remarkable. It can be deduced from this that the density of surface defects is increased considerably by the

sputter process. This is in accordance with older work,[16] where a strong fraction of up to 40% reduced Ti sites in the surface is reported.[15]

At these defect-rich surfaces the interaction with CO_2 molecules turns out to be quite different. The MIES spectra show a three-peak structure associated with a surface carbonate which is backed up by corresponding XPS results. Obviously, a surface carbonate is formed on top of the $SrTiO_3(100)$ surface. This could not be observed on the clean, unsputtered surfaces. It can be concluded that a high surface defect density is essential for the process.

Possibly, the reaction reads as follows:

$$2CO_2 \downarrow + V_O^{\bullet\bullet} + Ti_{Ti}'' \Rightarrow (CO_3)_O^{\times} + Ti_{Ti}^{\times} + CO \uparrow \qquad (3a)$$

This reaction includes the dissociation of a CO_2 molecule and the formation of a carbonate complex at a surface oxygen vacancy. The dissociation process is probably due to an electron transfer from the reduced titanium. The oxidation of the surface titanium in the reaction ($Ti_{Ti}'' \Rightarrow Ti_{Ti}^{\times}$) may be associated with the reduction of emission from corresponding 3d states just below the Fermi level in MIES.

In a previous study, it was shown that the main consequence of sputtering the surface is the breaking of surface Ti–O bonds.[16] This would make the reaction in Eqn (3a) plausible, as a surface oxygen vacancy and a neighbouring Ti^{2+} ion might be necessary for the production of the surface carbonate.

It has already been shown, that CO_2 can be dissociated in front of an $SrTiO_3(100)$ surface, supporting the view of a reaction according to Eqn (3a).[13]

Another imaginable reaction path is the involvement of a surface oxygen atom:

$$CO_2 \downarrow + Ti_{Ti}'' + O_O^{\times} + 2h^{\bullet} \Rightarrow (CO_3)_O^{\times} + Ti_{Ti}^{\times} \qquad (3b)$$

This reaction displays the direct formation of the carbonate at a surface oxygen atom from just one CO_2 molecule. Probably, electrons from the reduced surface titanium are required for an intermediate dissociation or activation process. Electronic holes $h^{\bullet}$ are available from the acceptor doping of the crystal.[31]

If one of these reaction paths is true, no dissociation products or other additional products should be detectable at the surface. In fact, no secondary carbon phase is detectable with XPS in Fig. 4 besides the carbonate. Of course, this would not rule out a dissociation process at the surface. Other studies concluded, that CO_2 can be dissociated in front of a sputtered $SrTiO_3$ surfaces.[15]

From the two possible reaction paths presented here Eqn (3a) seems to be more plausible, because it is backed up by results from previous studies and requires less unsupported presumptions. It is possible of course, that both reactions occur simultaneously.

The carbonate formation stops when all or almost all surface defects have been consumed by the reaction. This can be seen from the development of the CO_3^{2-} peak height in Fig. 9, which is a measure of the coverage of the surface with carbonate groups. A CO_2 exposure of about 200 L is necessary to reach saturation of the reaction. This is quite high, indicating a low reactivity of the surface to CO_2, at least from a surface science point of view.

The CO_3^{2-} peak height can be fitted with a Langmuir isotherm $\theta = 1 - \exp(-K\Gamma t)$, where θ is the relative coverage of the surface defects by CO_3^{2-} complexes, K is the reaction probability for CO_2 on the sputtered $SrTiO_3(100)$ surface and Γ is the number of CO_2 molecules impinging per surface defect and second. The exponent

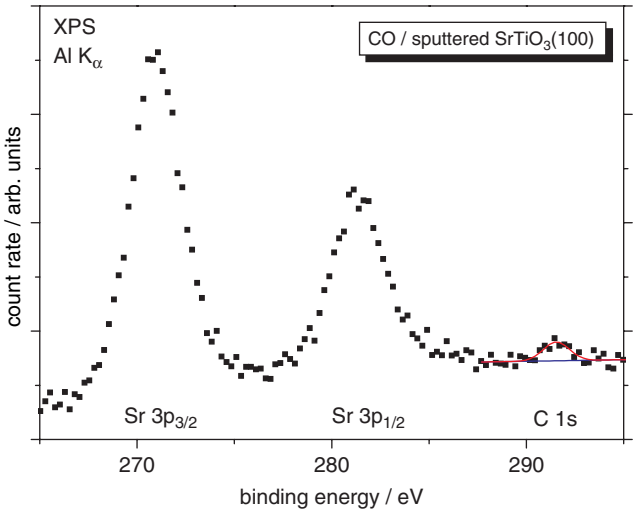

Figure 8. XPS spectrum of sputtered and CO exposed $SrTiO_3(100)$ (corresponding to the top MIES spectrum in Fig. 7) from the Sr 3p and C 1s region. The exposure amounts to 800 L CO.

contains the reaction probability K. Unfortunately, Γ is unknown to us quantitatively, so we can not unfold this information.

The WF changes linearly with the CO_3^{2-} formation. This means, that the WF change is only a function of the number of adsorbed dipoles on top of the surface. Because this linearity holds up to saturation, no dipole–dipole interaction must be taken into account for the WF change. Therefore, the CO_3^{2-} coverage of the surface must be only small.

When the carbonate covered $SrTiO_3$ crystal is heated to temperatures above 700 K (not shown here), the carbonate is desorbed from the surface completely. The desorption process has not been studied in detail, but is in accordance with reports from other groups.[15]

Surprisingly, carbonate formation on the $SrTiO_3$ surface could also be detected when the surface is exposed to CO. The MIES spectra in Fig. 7 as well as the XPS results from the O 1s region in Fig. 8 show the same structures as detected for the exposure to CO_2. This is not a contamination effect from CO_2 impurities in the CO gas, as can be deduced from mass spectrometry results. During the MIES experiment in Fig. 7, a total exposure of 800 L CO was offered to the surface. During the same period, the QMS shows the CO_2 exposure was well below 2.5 L. As can be seen in Fig. 3, this is much too less to explain the fully developed three-peak structure in MIES.

Possibly, the reaction occurs comparable to Eqn (3b):

$$CO \downarrow + Ti_{Ti}'' + 2O_O^{\times} + 4h^{\bullet} \Rightarrow (CO_3)_O^{\times} + Ti_{Ti}^{\times} + V_O^{\bullet\bullet} \qquad (4a)$$

This would require a diffusion of two surface oxygen ions to a surface defect Ti_{Ti}'', which would account for the lower reaction speed of the process compared to the reaction with CO_2.

Another thinkable reaction path would be to assume the source of the oxygen atoms needed for the CO_3^{2-} formation would be the gas phase:

$$3CO \downarrow + V_O^{\bullet\bullet} + Ti_{Ti}'' \Rightarrow (CO_3)_O^{\times} + Ti_{Ti}^{\times} + 2C \qquad (4b)$$

This reaction would include the dissociation of two CO molecules. The remaining two carbon atoms would stay at the surface.

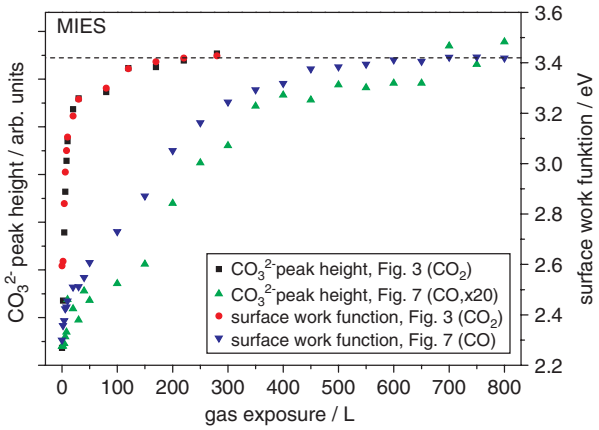

Figure 9. Peak height of the MIES experiments on sputtered $SrTiO_3$(100) exposed to CO_2 (squares, see Fig. 3) and CO (upward triangles, see Fig. 7) and surface WF of the same surfaces (circles and downward triangles) as a function of gas exposure.

Again, with our XPS setup no carbon atoms besides the carbonate can be detected, which would hint to a total dissociation of CO molecules in front of the surface. This does suggest the source of the additional oxygen atoms for the formation of the carbonate are not the CO molecules as depicted in Eqn (4b). Bearing this in mind, Eqn (4a) is much more plausible.

Of course, residual gas in the UHV chamber is a possible source of the required oxygen atoms for Eqn (4b). Water, for example, is known to be quite reactive with sputtered $SrTiO_3$(100) surfaces. However, it can be deduced from QMS that the H_2O partial pressure was even below the CO_2 partial pressure discussed above and certainly was below 2.5 L over the length of the experiment.

The CO offer of about 500 L necessary to reach saturation of the reaction is five times higher than the necessary CO_2 offer (Fig. 9). This indicates a much lower reactivity of the sputtered $SrTiO_3$ surface to CO. The CO_3^{2-} peak height for the CO exposed surface can be fitted with a Langmuir isotherm in the same way as described above for CO_2 exposure. However, the factor $K\Gamma$ is 40 times higher than for the CO_2 exposure. As the two sputtered $SrTiO_3$(100) surfaces used for the gas exposure experiments were prepared in the same manner, it is sure to assume that Γ is the same for both experiments. This indicates a drastically smaller reaction probability for the CO molecules on the sputtered $SrTiO_3$(100) surface than for the CO_2 molecules.

As for the CO_2 exposure, the WF changes linearly with the CO_3^{2-} formation when the surface is exposed to CO. When the reaction has reached saturation, both the CO_2 and the CO exposed surface exhibit the same WF of 3.42 eV, which is marked in Fig. 9.

Besides the different production process, the surface carbonate seems to be of the same type and quality and can be desorbed from the $SrTiO_3$ surface by heating to temperatures above 700 K as well.

Conclusions

Both the offer of CO_2 and CO to a cleaned $SrTiO_3$(100) surface does not lead to a change in surface electronic structure nor stoichiometry that would be detectable with MIES or XPS. On sputtered (100) surfaces, the exposure of the $SrTiO_3$ to both CO_2 and CO results in the formation of a surface carbonate CO_3^{2-}. The exposure to reach a saturation of the reaction is about 200 L for CO_2 and about 500 L for CO. The carbonate can be removed from the surface by annealing the surface to temperatures above 700 K.

Acknowledgement

The partial financial support by the Deutsche Forschungsgemeinschaft under contract nos. Ma 1893/9 and Ar 248/3 is gratefully acknowledged.

References

[1] R. Moos, T. Bischoff, W. Menesklou, K. H. Härdtl, *J. Mater. Sci.* **1997**, *32*, 4247.
[2] B. Stäuble-Pumpin, B. Ilge, V. C. Matjasevic, P. M. L. O. Scholte, A. J. Steinfort, F. Tuinstra, *Surf. Sci.* **1996**, *369*, 313.
[3] Y. Liang, D. A. Bonnell, *Surf. Sci.* **1994**, *310*, 128.
[4] V. Ravkiumar, D. Wolf, P. David, *Phys. Rev. Lett.* **1995**, *74*, 174.
[5] K. Szot, W. Speier, *Phys. Rev. B* **1999**, *60*, 5909.
[6] K. Szot, W. Speier, U. Breuer, R. Meyer, J. Szade, R. Waser, *Surf. Sci.* **2000**, *460*, 112.
[7] S. Steinsvik, R. Bugge, J. Gjønnes, J. Taftø, T. Norby, *J. Phys. Chem. Solid* **1997**, *58*, 969.
[8] G. M. Choi, H. J. Tuller, *J. Am. Ceram. Soc.* **1988**, *71*, 201.
[9] R. Moos, K. H. Härdtl, *J. Am. Ceram. Soc.* **1997**, *80*, 2549.
[10] N. H. Chan, R. K. Sharma, D. M. Smyth, *J. Electrochem. Soc.* **1981**, *128*, 1762.
[11] R. Merkle, J. Maier, *Angew. Chem. Int. Ed.* **2008**, *47*, 2.
[12] M. Leonhardt, R. A. de Souza, J. Claus, J. Maier, *J. Electrochem. Soc.* **2002**, *149*, J19.
[13] Chr. Argirusis, F. Voigts, P. Datta, J. Grosse-Brauckmann, W. Maus-Friedrichs, *PCCP* **2009**, *11*, 3152.
[14] J. D. Baniecki, M. Ishii, K. Kurihara, K. Yamanaka, T. Yano, K. Shinozaki, T. Imada, K. Nozaki, N. Kin, *Phys. Rev. B* **2008**, *78*, 195415.
[15] S. Azad, M. Engelhard, L. Wang, *J. Phys. Chem.* **2005**, *109*, 10327.
[16] F. Voigts, Chr. Argirusis, W. Maus-Friedrichs, *Surf. Interface Anal.* **2010**, DOI: 10.1002/sia.3681.
[17] M. Frerichs, F. Voigts, W. Maus-Friedrichs, *Appl. Surf. Sci.* **2006**, *253*, 950.
[18] J. H. Scofield, *J. Electron Spectrosc. Relat. Phenom.* **1976**, *8*, 129.
[19] National Institute of Standards and Technology. Electron inelastic-mean-free-path database 1.1, available at: http://www.nist.gov/srd/nist71.cfm. [Last accessed in 2011].
[20] Y. Harada, S. Masuda, H. Ozaki, *Chem. Rev.* **1997**, *97*, 1897.
[21] H. Morgner, *Adv. Atom. Mol. Opt. Phys.* **2000**, *42*, 387.
[22] G. Ertl, J. Küppers, in *Low Energy Electrons and Surface Chemistry*, VCH Verlag: Weinheim, **1985**.
[23] W. Maus-Friedrichs, M. Frerichs, A. Gunhold, S. Krischok, V. Kempter, G. Bihlmayer, *Surf. Sci.* **2002**, *515*, 499.
[24] F. Voigts, F. Bebensee, S. Dahle, K. Volgmann, W. Maus-Friedrichs, *Surf. Sci.* **2008**, *603*, 40.
[25] D. Ochs, B. Braun, W. Maus-Friedrichs, V. Kempter, *Surf. Sci.* **1998**, *417*, 406.
[26] P. A. W. van der Heide, *J. Electron Spectrosc. Relat. Phenom.* **2006**, *151*, 79.
[27] M. Frerichs, F. X. Schweiger, F. Voigts, S. Rudenkiy, W. Maus-Friedrichs, V. Kempter, *Surf. Interface Anal.* **2005**, *37*, 633.
[28] M. A. Henderson, *Surf. Sci.* **1998**, *400*, 203.
[29] U. Diebold, *Surf. Sci. Rep.* **2003**, *48*, 53.
[30] A. L. Linsebigler, G. Lu, J. T. Yates, *Chem. Rev.* **1995**, *95*, 735.
[31] R. Moos, K. H. Härtl, *J. Am. Ceram. Soc.* **1997**, *80*, 2549.

